Structure and Dynamics of Cold-Adapted Enzymes as Investigated by FT-IR Spectroscopy and MD. The Case of an Esterase from *Pseudoalteromonas haloplanktis*

Vincenzo Aurilia,[†,‡] Jean-François Rioux-Dubé,[‡,§] Anna Marabotti,[||] Michel Pézolet,[§] and Sabato D'Auria*[,†]

Laboratory for Molecular Sensing, Institute of Protein Biochemistry, CNR, Via Pietro Castellino, 111 80131 Naples, Italy, Centre de Recherche sur les Matériaux Avancés, Département de Chimie, Université Laval, Québec, Québec, Canada G1 V 0A6, and Laboratory of Bioinformatics, Institute of Food Sciences, CNR, Avellino, Italy

Received: March 2, 2009; Revised Manuscript Received: April 15, 2009

Psychrophiles are cold-adapted organisms that produce enzymes that display a high catalytic efficiency at low temperatures. In recent years, these low-temperature working enzymes have attracted the attention of scientists because of their peculiar properties that render them particularly useful in investigating the relationship between enzyme stability and flexibility. Recently, a new esterase was identified and isolated from the cold-adapted organism *Pseudoalteromonas haloplanktis*. The enzyme, denoted as PhEST, presents a dimeric structure with a molecular mass of 60 kDa. In this work, we used Fourier transform infrared spectroscopy and molecular dynamics simulations to investigate the functional and structural properties of PhEST over a wide range of temperature. The obtained results reveal that the structure of PhEST is quite stable up to 40 °C. In fact, the protein starts to denature at about 45 °C through the formation of new secondary structural elements such as intermolecular β-sheets. In addition, our results indicate that the flexibility of protein segment 55−65 (335−345 in subunit B), which corresponds to a loop near the active site of the enzyme, plays a crucial role in the protein function.

Introduction

Extremophiles are organisms living and thriving under conditions considered "extreme" for the human life. For example, temperature-based extremophiles consist of organisms living at low temperatures (psychrophiles) and organisms living at high temperatures (thermophiles). Several studies have been performed on thermophilic organisms.[1] In particular, in recent years, much interest has focused on the study of the molecular strategies adopted by these enzymes and proteins to work in very harsh environments.[2−4] It is widely believed that it is fundamental to acquire knowledge on the molecular mechanisms that rule the relationship between stability, flexibility, and activity in enzymes from extremophiles to shed light on the protein folding, unfolding, and misfolding processes that occur in the cell life cycle. In fact, the increasing number of three-dimensional (3D) structures of enzymes and proteins from thermophiles has shed light on the molecular determinants of their structural stability. One of the most relevant differences found when comparing the 3D structures of proteins from thermophiles with their mesophilic counterparts is an increased number of ion pairs organized in large networks that confer more structural rigidity to the enzyme and, in turn, more stability at high temperatures.[5] The relationship among rigidity, stability, and activity has always been of fundamental interest for relating enzyme activity to enzyme stability. Tang and Dill investigated the temperature-induced fluctuations in a lattice model,[6] and their studies pointed out that proteins having greater stability tend to have fewer large fluctuations and, hence, lower flexibility.[6] By translating the results obtained on lattice model to biomolecules, it is possible to state that, if flexibility is a fundamental feature to have efficient enzyme catalysis, this would explain why enzymes from thermophilic organisms, which are exceptionally stable at high temperatures, are almost catalytically inactive at normal temperatures.

In a recent article, we described the isolation and purification of an esterase isolated from the antarctic organism *Pseudoaltermonas haloplanktis* TAC125 (PhEST). PhEST presents a dimeric structure with a molecular mass of 60 kDa and exhibits an optimum activity at 20 °C.[7]

In this work, we probed the effect of temperature on the stability and flexibility of this cold-adapted enzyme by Fourier transform infrared (FT-IR) spectroscopy and molecular dynamics (MD) simulations. The obtained results reveal that the structure of PhEST is quite stable up to 40 °C and that the flexibility of protein segment 55−65 (335−345 in subunit B), which corresponds to a loop near the active site of the enzyme, plays a crucial role in the protein function.

Materials and Methods

Bacterial Strains, Plasmids and Growth Conditions. *P. haloplanktis* TAC125[8] was grown to saturation at 4 °C in TYP broth (16 g L^{-1} yeast extract, 16 g L^{-1} bacto-tryptone, and 10 g L^{-1} sea salts at pH 7.5). The *E. coli* strains used in this study were TOP10F′ (Invitrogen, Carlsbad, CA) and BL21(DE3) (Novagen, San Diego, CA). The plasmids used for cloning the esterase were pGEM-T (Promega, Madison, WI) and pET28a (Novagen). Recombinant *E. coli* strains were cultured at 37 °C in Luria−Bertani broth supplemented with ampicillin or kanamycin.

* Corresponding author. Phone: +39-0816132250. Fax: +39-0816132277. E-mail: s.dauria@ibp.cnr.it.
[†] Institute of Protein Biochemistry, CNR.
[‡] V. Aurilia and J. F. Rioux-Dubé contributed equally to this work.
[§] Université Laval.
[||] Institute of Food Sciences, CNR.

10.1021/jp901921r CCC: $40.75
Published on Web 05/12/2009

Isolation of the Esterase Gene from *P. haloplanktis* TAC125. Genomic DNA from *P. haloplanktis* was extracted from bacterial cells using the commercial kit Wizard Genomic DNA prep supplied from Promega. The gene encoding an esterase (PSHAa 1385) was amplified by polymerase chain reaction (PCR) using two primers that define the N-terminal and C-terminal regions of the gene. The 5′ primer used in the amplification contained the ATG start codon and a *Bam*HI site (indicated by bold and underlined characters, respectively, in the sequence): PA1385FW: TAGGATCCGGC**ATG**TTAGAAAATATCTCAAGTG.

The 3′ primer PA1385RV1 had the following sequence: 5′-AGGCTCGAGAAATCCT**AAT**AGTTATGCAGAC-3′ and was designed to insert a recognition site for the *XhoI* endonuclease (underlined) immediately upstream of the termination codon (bold characters). The reaction was performed in a Mastercycle apparatus using *Taq* polymerase High Fidelity (La Roche, Mannheim, Germany) as the enzyme under the following conditions: denaturation at 95 °C for 5 min, followed by 30 cycles of denaturation at 95 °C for 1 min, annealing at 55 °C for 1 min, and extension at 72 °C for 1 min. The resulting DNA fragment was ligated into the pGEM-T plasmid and DNA fragments from 10 independent clones, and it was sequenced (PRIMM, Seq core, Naples, Italy) to ensure that no mutation had occurred during the amplification. The gene PSHAa 1385 was then excised from the plasmid pGEM-T using *Bam*HI and *XhoI* restriction enzymes, separated on a 1.0% agarose gel, and purified using a DNA gel extraction kit purchased from Stratagene (La Jolla, CA). The fragment obtained was ligated into pET28a expression vector digested with the same enzymes so that a six-histidine stretch was fused at the N-terminus of the recombinant module.

Protein Expression. N-terminus His6-S-tagged protein constructs from pET28a were overexpressed following transformation in *E. coli* BL21 (DE3). Cells were recovered and lysed by sonication (Soniprep, Sanyo) after growth at 37 °C in Luria−Bertani medium supplemented with kanamycin. Induction was carried out by adding 0.1 mM isopropyl-β-D-thiogalactopyranoside (IPTG) to a culture at an optical density of 0.5 measured at 600 nm and then incubating the culture at 37 °C for 3 h. Protein constructs were purified by nickel affinity chromatography as described by the manufacturer (Novagen). Thrombin cutting on a column was used to obtain the protein without the His stretch at its N-terminus. The purified protein was analyzed by SDS-PAGE (sodium dodecyl sulfate polyacrylamide gel electrophoresis) and by Western Blotting with anti-His antibodies.

Protein Determination and Enzyme Assay. Protein concentration was determined using the BioRad protein staining assay, with bovine serum albumin (BSA) as the standard. The esterase activity was determined at temperatures ranging from 5 to 50 °C using *p*-nitrophenyl acetate (*p*NPAc) as the substrate. The assay mixture (1 mL final volume), contains 5 mM *p*NPAc in 20 mM sodium phosphate buffer at pH 7.4, and the assay started by adding the enzyme sample to the mixture. The release of *p*-nitrophenol was continuously monitored at 405 nm by a Cary ultraviolet−visible spectrophotometer equipped with a dual-cell Peltier temperature controller (Varian, Palo Alto, CA). One enzyme unit was defined as the amount of enzyme releasing 1 μmol of *p*-nitrophenol per minute under the described conditions. Assays using α- and β-naphthyl acetate were analyzed following the release of α- and β-naphtol, respectively, monitored at 560 nm.[7]

Infrared Spectroscopy. Fourier transform infrared spectroscopy was used to investigate the PhEST protein stability and heat-induced secondary structure changes. The protein was dissolved directly in D_2O (CDN Isotopes, Sainte-Claire, PQ, Canada) for 1 h at a concentration of 0.45 mg/mL. To eliminate the high concentration of salts in the sample and to increase the protein concentration, the samples were centrifuged at 6000*g* through Amicon Ultra-4 (10 kDa) (Millipore, Billerica, MA) filters. A volume of 20 μL of the protein solution was deposited between the two CaF_2 windows of a Biocell from Biotools, Inc. (Jupiter, FL) manufactured with a calibrated path length of 40 μm. The transmission spectra were recorded at a resolution of 2 cm^{-1} using a Nicolet Magna 560 spectrometer (Thermo Electron Corporation, Madison, WI) equipped with a narrow-band mercury cadmium telluride (MCT) detector and continuously purged with dry air. For each spectrum, 128 scans were coadded and apodized with a Happ−Genzel function. The sample temperature was computer-controlled using an Omega temperature controller (Stamford, CT) and Peltier elements. Spectra were recorded at 2, 4, 5, 10, 15, 20, 25, 30, 35, 40, 45, 50, 55, 60, 65, 70, 75, and 80 °C with an equilibration period of 5 min at each desired temperature. The whole data treatment of the amide I′ band was made with Grams/AI 8.0 software (Thermo Electron Corporation, Waltham, MA). Water vapor was subtracted, the subtraction factor being optimized using the autosubtract function. For each temperature, the spectrum of D_2O at the same temperature was subtracted from that of the protein solution. For the study of the amide I′ region, a linear baseline was drawn between 1730 and 1580 cm^{-1}. All spectra were normalized to obtain an area of 1 for the amide I′ band. Difference spectra were calculated by subtracting the spectrum recorded at 2 °C from all other spectra using a subtraction factor of 1. Fourier deconvolution of the amide I′ region was done in Grams/AI using the method of Griffiths and Pariente[9] with a narrowing parameter, γ, of 7 and a 94% Bessel smoothing function. These parameters were chosen to obtain enough band narrowing to see the major components of the amide I′ band but without introducing significant side lobes in the 1690−1720 cm^{-1} region where there is no protein band. The experiments were repeated three times and were reproducible.

Modeling of PhEST Structure. The structure of monomeric PhEST was predicted by homology modeling methods using the program MODELER version 6.1[10] implemented in the molecular simulation package InsightII (version 2000.1, Accelrys, Inc., San Diego, CA, 2000). The structure of *Saccharomyces cerevisiae* S-formylglutathione hydrolase,[11] available in the PDB database[12] (PDB code 1PV1), was selected as a suitable template after a BLAST search[13] and a further confirmation using the fold recognition servers SAM-T02[14] and FUGUE.[15] To improve the alignment of the two proteins using information on common features of the protein family, the sequences of target and templates were first aligned with each other and with those of the first 30 carboxylesterases and formylglutathione hydrolases found with a BLAST search on the UniProt/SwissProt database[16] using the program T-Coffee.[17] The PredictProtein server[18] was then used to perform predictions on the type and position of secondary structure elements on PhEST, which were compared with those present on the template and calculated using DSSP.[19] Few manual adjustments to avoid the placement of gaps within the segments of secondary structure were finally performed before subjecting the alignment to the following steps.

With the program MODELER, we created 10 different models of PhEST, and we chose the best one by analyzing their stereochemical properties and their overall quality with the programs PROCHECK[20] and ProsaII.[21] The stereochemical

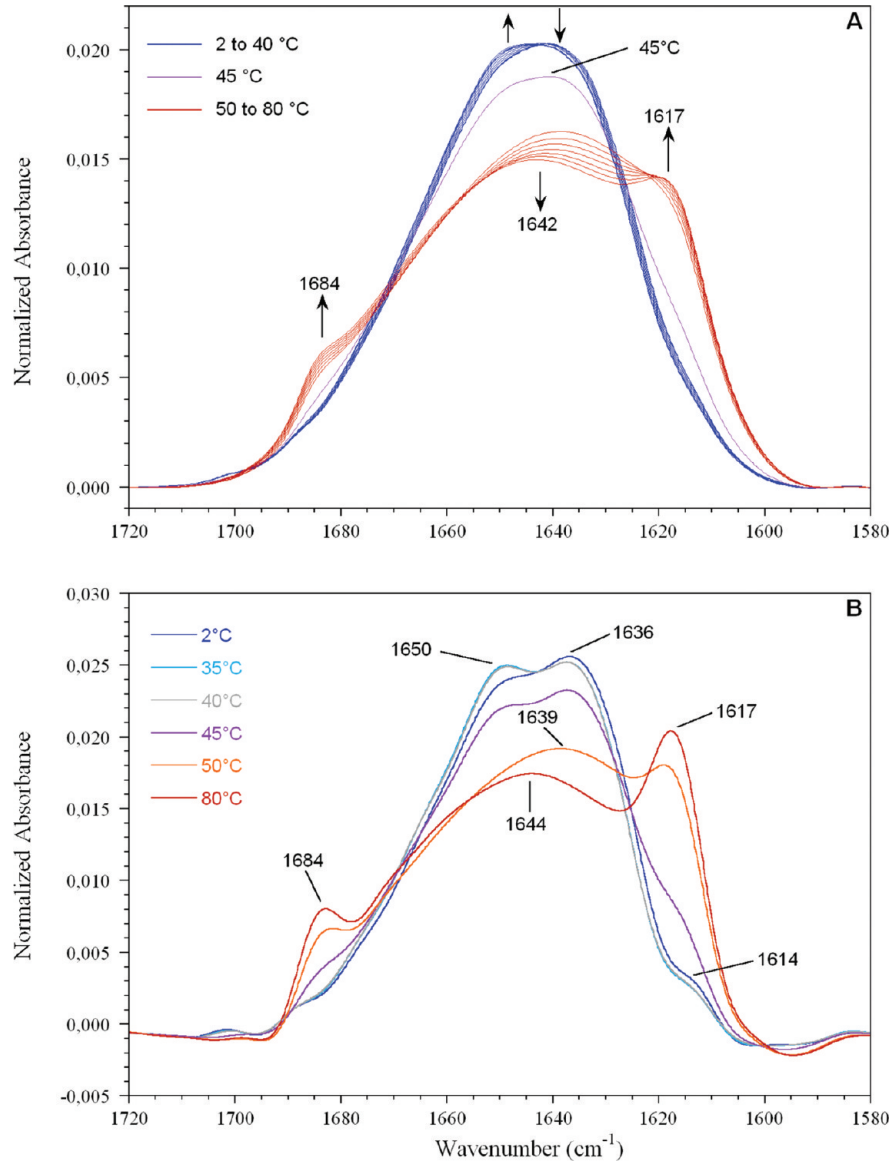

Figure 1. (A) Infrared spectra in the amide I′ region of PhEST between 2 and 80 °C (see Materials and Methods for the list of all studied temperatures). Arrows indicate the direction of spectral changes as the temperature increases. (B) Fourier deconvolved spectra in the amide I′ region of PhEST at 2, 35, 40, 45, 50, and 80 °C.

parameters of the best monomeric model obtained for PhEST showed 86.5% of the residues in the most favored regions of the Ramachandran plot and only 0.8% of residues in disallowed regions (the analysis performed on the template showed 80.4% and 1.2% of residues for most favored and disallowed regions, respectively). The ProsaII z score (−10.07) is also in the range of scores typically found in proteins of similar sequence length[21] and is very similar to that of template (−10.58). These data indicate that the model we obtained is of good quality (even better than the template for stereochemical properties).

The model of the dimeric structure of PhEST was created by superimposing two monomeric chains onto the structure of a dimer of *Saccharomyces cerevisiae* S-formylglutathione hydrolase, with the aid of InsightII tools. Then, a mild optimization was applied to reduce steric clashes using 500 steps of the steepest-descent method, with a final gradient of 0.01 kcal/mol. The CVFF (Consistent Valence Force Field) developed for InsightII was used to assign potentials and charges. All atoms were allowed to relax with no constraints. This procedure represents the best compromise between the need for relieving steric clashes and the risk of distorting the geometry of the protein with deep and extensive minimization. The control of the final quality of the dimer was performed again with PROCHECK and ProsaII. The quality of the dimeric models in terms of stereochemical parameters was similar to that of the original monomeric model (85.7% and 0.4% of residues in most favored and disallowed regions of the Ramachandran plot, respectively), and in addition, the minimization decreased the z score (−10.57), indicating an improvement of the overall quality of the model.

Molecular Dynamics Simulations and Analysis of the Results. Molecular dynamics (MD) simulations were carried out using the program GROMACS version 3.3.1[22,23] running in parallel (MPI) on a cluster with 40 × 86_64 Opteron processors. The GROMOS96 force field[24] was used throughout the simulations. The dimeric protein was included in a triclinic box with a distance of 0.75 nm per side from the protein, filled with 12034 water molecules [Simple Point Charge (SPC) model[25]] and 15 Na^+ ions added to neutralize the net negative charge of the whole system, replacing the corresponding number of water molecules, with the aid of GROMACS utilities. Periodic boundary conditions were used to exclude surface effects.

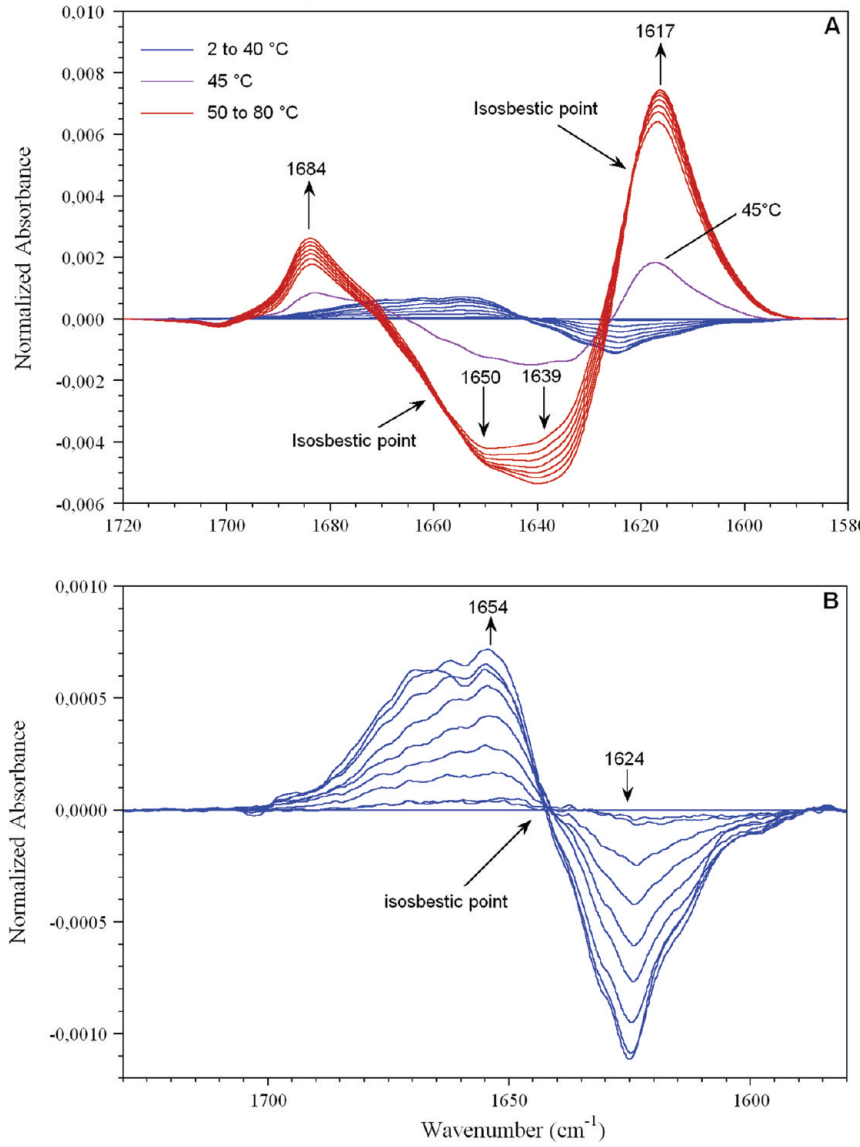

Figure 2. Difference spectra in the amide I′ region of PhEST (A) between 2 and 80 °C and (B) between 2 and 40 °C (see Materials and Methods for the list of all studied temperatures). Arrows indicate the direction of spectral changes as the temperature increases.

A preliminary energy minimization step with a tolerance of 1000 kJ mol^{-1} nm^{-1} was run with the steepest-descent method. All bonds were constrained using LINCS.[26] After minimization, a short MD simulation (20 ps) with position constraints was applied to each system to soak the solvent into the macromolecule. A time step of 2 fs was used in all cases, and the systems were coupled to a temperature bath at 300 K and to a pressure of 1 atm using Berendsen's method.[27] Long-range electrostatics were handled using the particle-mesh Ewald (PME) method.[28] Cutoffs were set at 0.9 nm for Coulomb interactions and at 1.4 nm for van der Waals interactions. Finally, three 10-ns-long simulations, one each at 4, 20, and 45 °C, were performed with a time step of 2 fs and without any position constraints.

After that, several analyses were conducted using programs built within GROMACS package, and the results were visualized and elaborated with the aid of the freely available program Grace (http://plasma-gate.weizmann.ac.il/Grace). The energy components were extracted from the energy files generated by the program and analyzed to verify the stabilization of the system. For each simulation, an "average" structure representative of the trajectory was calculated, not including hydrogen atoms. These average structures were saved in pdb format and were subsequently minimized with the steepest-descent method as described above. Visualization and analysis of model features were carried out using InsightII facilities.

The percentage of residues embedded in secondary structure elements and their variation during the simulations were evaluated using the program DSSP.[19] H-bonds were calculated with HBPLUS.[29] Identification of salt bridges was done directly on average minimized structures obtained as described above, using the criteria by Kumar and Nussinov.[30]

Results and Discussion

Infrared Spectroscopy. Figure 1A shows the transmission infrared spectra of PhEST in D_2O at different temperatures from 2 to 80 °C in the 1580−1720 cm^{-1} spectral region. The strong band between 1600 and 1700 cm^{-1} is due to the amide I′ vibration, a mode that is sensitive to the protein secondary structure.[31] At 2 °C, the amide I′ band is quite broad (47 cm^{-1}) and centered at 1642 cm^{-1}, indicating that the secondary structure of PhEST is composed of several conformations that give unresolved amide I′ components. Fourier deconvolution of the amide I′ band (Figure 1B), however, reveals two

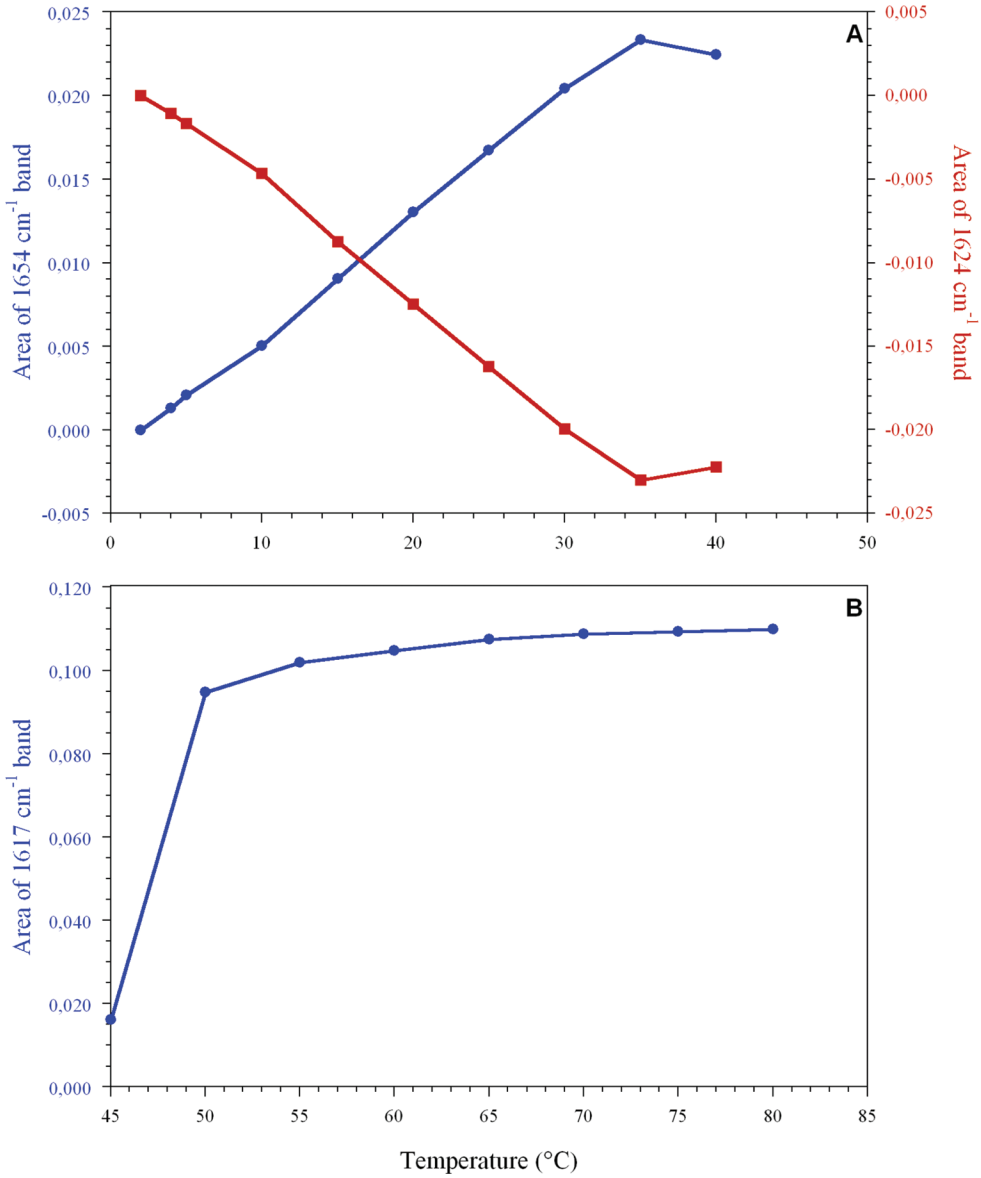

Figure 3. Effect of temperature on the intensity of the amide I′ components in the difference spectra of PhEST. Evolution of the areas of (A) the 1624 and 1654 cm^{-1} components at low temperatures between 2 to 40 °C and (B) the 1617 cm^{-1} component at high temperatures between 40 to 80 °C.

components of almost equal intensity at 1636 and 1650 cm^{-1} that are assigned to β-strands and α-helices, respectively.[31−34] This result is in agreement with the three-dimensional structure of the protein that shows that the protein backbone is composed of a central β-sheet surrounded by α-helices.[35,36] The relatively high wavenumber position of the 1636 cm^{-1} band suggests weak hydrogen bonding for the β-strands. As seen in Figure 1A, PhEST undergoes two different conformational transitions as the temperature is increased. Between 2 and 45 °C, the protein is quite stable, and only minor changes in secondary structure occur. On the contrary, at temperatures above 45 °C, major spectral modifications are observed. To better highlight these changes, difference spectra were calculated by subtracting the spectrum recorded at 2 °C from the spectra recorded at all other temperatures.

As seen in Figure 2A, the difference spectra clearly show that, above 40 °C, bands at 1617 and 1684 cm^{-1} increase in intensity with temperature whereas the intensity components at 1639 and 1650 cm^{-1} concomitantly decreases. The bands at 1617 and 1684 cm^{-1} are highly characteristic of the presence of antiparallel intermolecular β-sheets formed by temperature-induced self-aggregation of proteins.[37−40] The presence of isosbestic points at 1622 and 1658 cm^{-1} in the difference spectra indicates that the conversion of the β-strands and helices into intermolecular β-sheets is a two-state equilibrium process.

To emphasize the changes of the PhEST secondary structure at low temperature, the difference spectra from 2 to 40 °C are enlarged in Figure 2B. This figure shows that, as the temperature is increased, a band at 1624 cm^{-1} assigned to β-strands[40] decreases in intensity whereas a broad component located at approximately 1654 cm^{-1} assigned to the unordered conformation increases in intensity.[34] The integrated intensities of these bands in the difference spectra correspond to about 1% and 2%, respectively, of the total intensity of the amide I band at 20 and 40 °C. These results thus show that, between 2 and 40 °C, the native-structure PhEST is quite stable and only partly unfolds as some intramolecular hydrogen bonds of β-strands are broken. The isosbestic point observed at 1642 cm^{-1} also indicates that this conformational transition is a two-state equilibrium process.

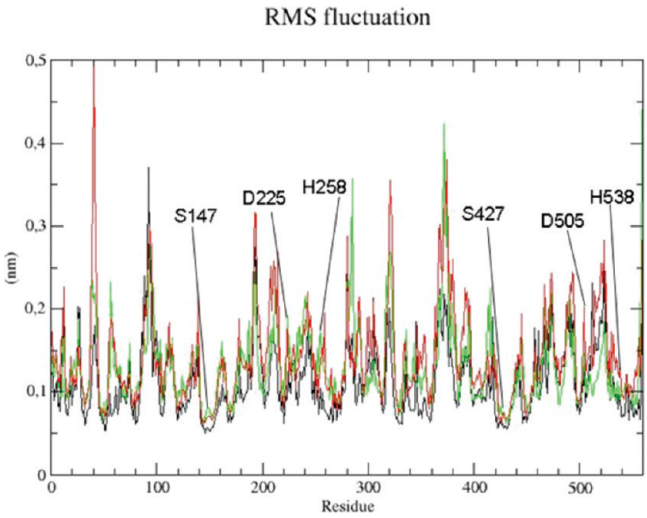

Figure 4. Root-mean-square fluctuations (RMSFs) of the residues in PhEST during MD simulations at temperatures of 4 °C (black), 20 °C (green), and 45 °C (red). The peaks corresponding to the residues belonging to the active sites in the two subunits are labeled.

Figure 3A presents the effect of temperature on the area of the 1624 and 1654 cm^{-1} components for the low-temperature conformational transition. As can be seen, the unfolding of the PhEST protein between 2 and 35 °C is not cooperative but rather is gradual, the transition being almost linear. The unfolding of the PhEST protein seems to be completed around 35 °C, which is close to the temperature of the maximal activity of the PhEST protein.[7] At higher temperatures, the unfolded protein starts to self-aggregate into antiparallel intermolecular β-sheets, and this process occurs abruptly around 40 °C and is completed at 50 °C, as revealed by evolution of the area of the 1617 cm^{-1} component (Figure 3B).

Molecular Dynamics Simulations. Three molecular dynamics (MD) simulations were carried out at 4 °C (optimal growth temperature for the bacterium), 20 °C (optimal temperature for enzymatic activity), and 45 °C (limiting temperature for the native state determined from the infrared results), starting from the model of dimeric PhEST created as described in Materials and Methods (see above). During these simulations, the two subunits of the protein remained associated. The total energy and its components (potential and kinetic energies) and the temperature were stable during each simulation, and the equilibrium was reached in less than 5 ps. The radius of gyration of the protein was stable at 4 °C and slightly decreasing at 20 and 45 °C, as was the solvent-accessible surface area (SASA) (data not shown). Analysis of the three average minimized structures obtained after the simulations at three different temperatures shows that there are no major changes of the secondary structure of PhEST between 4 and 45 °C, and in particular, the percentages of secondary structures are almost constant between 4 and 20 °C. The percentage of helices varies only from 29% at 4 °C to 30% at 45 °C, in agreement with the infrared results that indicate that the variation of the amide I′ intensity is only 1% for this temperature range. The percentage of β-sheets decreases from 20% to 19% between 4 and 20 °C, and it increases to 22% at 45 °C, in agreement with the infrared results showing that the amount of β-sheets decreases slightly as the protein unfolds and increases as the protein aggregates at high temperature.

We also determined whether the temperature can influence the activity of the enzyme via structural modifications and/or increased flexibility at molecular level. The root-mean-square fluctuations (RMSFs) of the atomic positions of PhEST at different temperatures are shown in Figure 4. The number of fluctuating residues increases at increasing temperature, as expected. It is possible to identify several zones of the enzyme characterized by significant mobility, corresponding to flexible loops joining segments of secondary structures. One of these zones is segment 55−65 (335−345 in subunit B), which corresponds to a loop positioned less than 10 Å far from the active site. Interestingly, this segment shows an enhanced fluctuation at 20 °C that is lower at 45 °C and practically absent at 4 °C. Considering other segments surrounding the active site (less than 10 Å from the catalytic triad), it is possible to see a variation of RMSFs under the three different temperature conditions. In particular, residues 180−190 and 250−265 in subunit A (corresponding to residues 460−470 and 530−545 in subunit B) appear to be more flexible at temperatures higher than 4 °C (Figure 4). Residues 180−190 form a helix on top of the active site, and segment 250−265 includes H258, which belongs to the catalytic triad. Considering the RMSFs of the three catalytic residues, S147 (S427) is one of the least fluctuating residues in the protein under any conditions, whereas the RMSFs of D225 (D505) and H258 (H538) are considerably higher at high temperatures. This observation suggests a molecular explanation for the activation of the enzyme at 20 °C.[7] The gain in flexibility of these segments might favor the entry of substrates and/or catalysis, whereas at low temperature, the active site of the protein shows a more rigid conformation and the catalysis slows. In addition, the fact that the peaks observed in Figure 4 at residue positions around 40 and 320 are located in loops joining β-strands further supports the results obtained by infrared spectroscopy.

We also analyzed the variation of the distance between D225 (D505) and H258 (H538) during the simulations, by measuring the distances between the two oxygen atoms of the carboxylic moiety of Asp and ND1 of His (Figure 5). At 4 and 20 °C, the distance appears to be quite stable, whereas at 45 °C, there are major fluctuations. Thus, it is possible to infer that excessive flexibility of the protein caused by high temperatures impairs the correct activity of the enzyme. In fact, the well-known mechanism of the catalytic triad requires the formation of an interaction between ND1 of His and the carboxylic moiety of Asp to ensure the right charge state of the imidazole ring: if this H-bond is not stable, the enzyme will be less active. We also used the program HBPLUS[29] to detect the presence of this bond in the average minimized structures, and we found an interaction between the side chains of D225 and H258 only at 20 °C, whereas at the other temperatures, this bond was not present. Therefore, from these simulations, it seems that the reason for the low activity of PhEST at 4 °C is the lack of the proper flexibility of the structures around the active site, whereas at 45 °C, the reason is the lack of proper interactions among the residues of the catalytic triad.

We also performed an analysis of the salt bridges present in the average minimized structures at the three different temperatures. The results are listed in Table 1.

There are many more ion pairs at low temperature than at high temperature, but eight of these pairs are also conserved at high temperatures, suggesting a crucial role in stabilizing this enzyme. In fact, as can be noted in Figure 6, four of the eight ion pairs conserved under all conditions bring together the two subunits of the protein. Two ion pairs (E59−K344 and E339−K64) are grouped together in the perfect middle of the dimer, and two others (D548−K69 and D268−K349) are in the "close" part of the dimer, on the opposite side from the

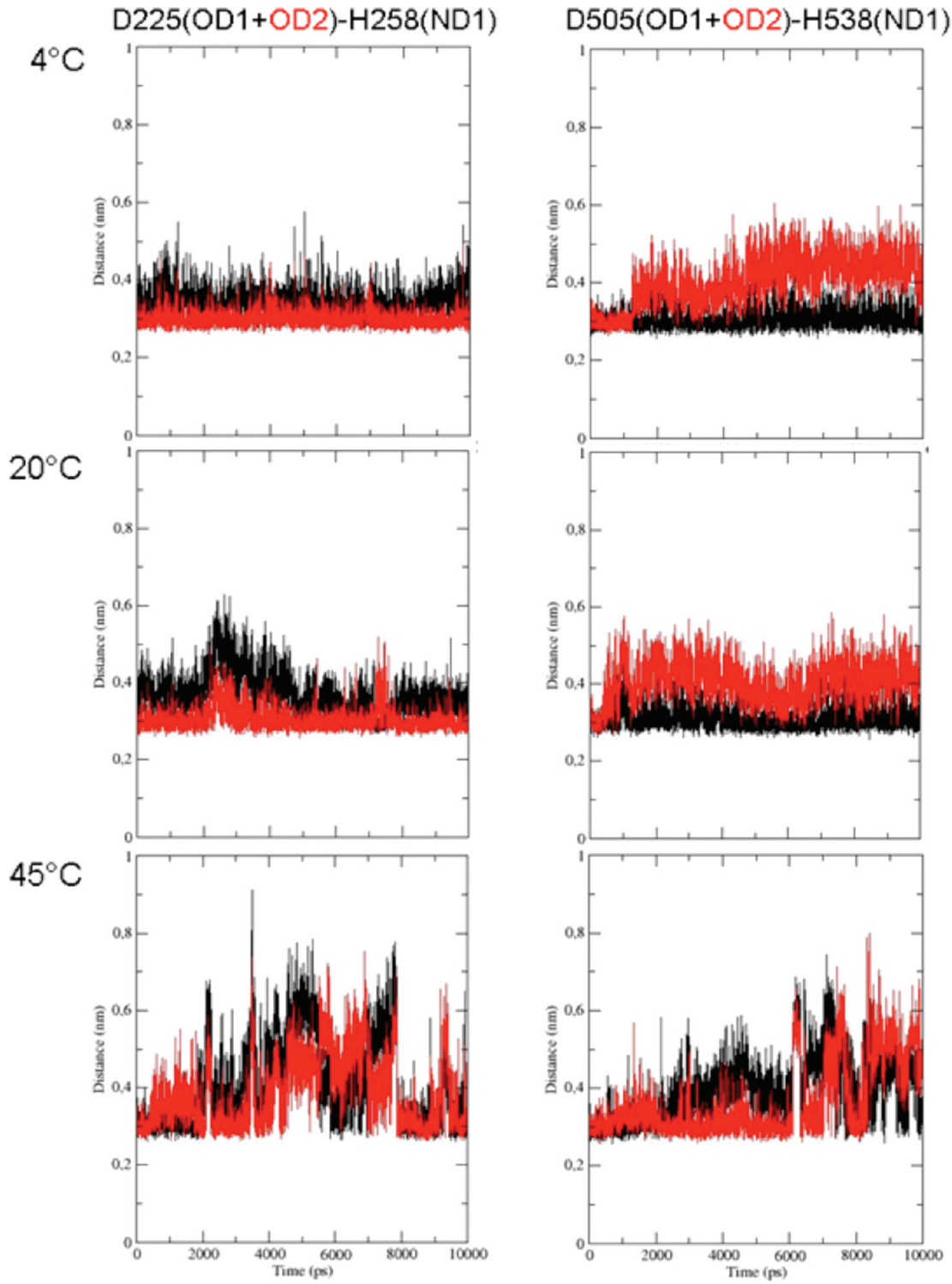

Figure 5. Variation of the distance between the pairs (A) D225−H258 and (B) D505−H538 during the simulations at 4, 20, and 45 °C. We measured the distances between the two oxygen atoms of the carboxylic moiety of Asp and ND1 of His. In black are the variations in the distance between Asp225/505−OD1 and His258/538−ND1. In red are the variations in the distance between Asp225/505−OD2 and His258/538−ND1.

active sites. Two other symmetrical ion pairs (D97−K184 in subunit A, D377−K464 in subunit B) bring together a helix and a loop on the top of the active site and might play some functional roles in the enzyme. It is noteworthy that these ion pairs connect two of the most flexible segments of the protein and segments whose motility seems to be influenced by high temperatures (see above and Figure 4). Probably the loss of this interaction would result in an excessive motility of this part of molecule, with a severe impairment of the catalytic activity. In addition, the last two ion pairs (E73−K69 and D481−K484) seem not to have a crucial role, being involved in intrahelical interactions.

Among the other salt bridges lost at high temperatures, some of them involve interactions within the helices, and others are formed by residues included in the β-strands. In particular, the interaction in the E283−K296 residue brings together the two first strands of the β-sheet in subunit B of the enzyme, and each of the interactions D58−R30, D82−R86, D163−K141, and

TABLE 1: Ion Pairs in the Average Minimized Structure of PhEST at Different Temperatures[a]

4 °C	20 °C	45 °C
E59−K344	**E59−K344**	**E59−K344**
E73−K69	**E73−K69**	**E73−K69**
E283−K296	**E339−K64**	**E339−K64**
E339−K64	E353−K350	**D97−K184**
E339−K344	**D97−K184**	D163−K141
E353−K70	D201−K204	D229−K233
E353−K350	D229−K233	**D268−K349**
E353−K349	**D268−K349**	**D377−K464**
E490−K488	D268−K70	**D481−K484**
E510−K513	**D377−K464**	**D548−K69**
D97−K184	D443−K421	D338−R310
D121−K159	**D481−K484**	
D163−K141	**D548−K69**	
D201−K204	D338−R310	
D245−K244		
D268−K349		
D377−K464		
D481−K484		
D509−K513		
D548−K69		
D548−K350		
D58−R30		
D82−R86		
D362−R366		

[a] Ion pairs present in all average structures at different temperatures are highlighted in bold.

D362−R366 includes one residue belonging to a β-strand and placed especially at either end of the secondary structure.

Conclusions

Psychrophiles are organisms that produce cold-evolved enzymes that display a high catalytic efficiency, associated with a low thermal stability. PhEST is a cold-adapted protein that presents a dimeric structure with a molecular mass of 60 kDa. PhEST was crystallized, and its three-dimensional structure was solved at 2.10 Å.[35] Preliminary data indicate that the enzyme exhibits a globular structure consisting of a nine-stranded mixed β-sheet, with the first and third strands running antiparallel to the others. The β-sheet is surrounded by nine α-helices and exhibits a pronounced twist, with approximately a 90° angle between the first and last strands. In addition, the residues constituting the catalytic triad (Ser 147, Asp 225, and His 258) and those forming the so-called oxyanion hole (Leu54 and Met148) were identified.[35]

Results from the infrared spectroscopy experiments and molecular dynamics simulations performed in this work point out that the conformation of PhEST is quite stable between 2 and 40 °C. In particular, the infrared results indicate that the protein denatures near 45 °C with the formation of intermolecular β-sheets. The infrared results further reveal that the protein partly unfolds between 2 and 40 °C with a slight loss of some β-strands.

Molecular dynamics simulations results suggest that, as expected, the flexibility of the protein structure increases with temperature increasing. Interestingly, the fluctuation of protein segment 55−65 (335−345 in subunit B), which corresponds to a loop near the active site of the enzyme, is very small at 4 °C, increases at 20 °C, and decreases at 45 °C, supporting the fact that the optimal temperature for enzymatic activity is at around 20 °C. In addition, the hydrogen bond between residues D225 and H258, which belong to the catalytic triad, is found only at 20 °C. These results thus suggest that the flexibility of the protein strongly affects its catalytic activity, the protein being too rigid at 4 °C and too flexible at 45 °C to allow proper interactions between the residues of the catalytic site.

Finally, the MD results also indicate that the number of salt bridges, which decreases with temperature, is of fundamental importance in maintaining the structural integrity of the protein structure. The fact that some of the broken bridges involve residues in β-strands supports the partial loss of this conformation as observed by infrared spectroscopy.

Acknowledgment. This project was realized within the framework of the CNR Commessa "Diagnostica Avanzata ed Alimentazione". The authors are indebted to Prof. Mariorosario Masullo and Prof. Paolo Arcari from the Dipartimento di Biochimica e Biotecnologie Mediche, Università di Napoli Federico II, via S. Pansini 5, 80131 Napoli, Italy, for providing the biomass of *Pseudoalteromonas haloplanktis* and to Dr.

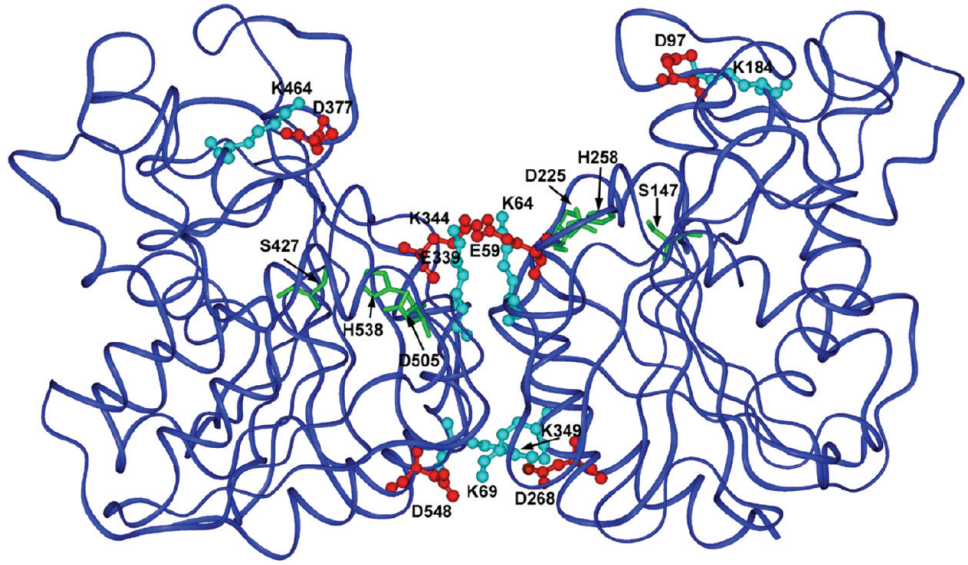

Figure 6. Schematic representation of the positions of conserved ion pairs in the structure of dimeric PhEST. The backbone of the protein is represented in ribbons. Residues belonging to the active sites of the two subunits are represented in stick mode and colored green. Residues forming the ion pairs are represented in ball-and-stick mode (cyan, basic residues; red, acidic residues) and labeled.

Umberto Amato for hosting MD simulations on the cluster "Lilligrid" located at the IAC-CNR, Naples, Italy. This work was also partially supported by the CNR-Bioinformatics project.

References and Notes

(1) Stetter, K. O.; Fiala, G.; Huber, R.; Huber, A.; Segerer, A. *FEMS Microbiol. Lett.* **1990**, *75*, 117.

(2) Van den Burg, B.; Vriend, G.; Veltman, O. R.; Venema, G.; Eijsink, V. G. *Proc. Natl. Acad. Sci. U.S.A.* **1998**, *95*, 2056.

(3) Kraut, J. *Science* **1988**, *242*, 533.

(4) Goldman, A. *Structure* **1995**, *3*, 1277.

(5) Yip, K. S.; Stillman, T. J.; Britton, K. L.; Artymiuk, P. J.; Baker, P. J.; Sedelnikova, S. E.; Engel, P. C.; Pasquo, A.; Chiaraluce, R.; Consalvi, V.; Scandurra, R.; Rice, D. W. *Structure* **1995**, *3*, 1147.

(6) Tang, K. E.; Dill, K. A. *J. Biomol. Struct. Dyn.* **1998**, *16*, 397.

(7) Aurilia, V.; Parracino, A.; Saviano, M.; Rossi, M.; D'Auria, S. *Gene* **2007**, *397*, 51.

(8) Médigue, C.; et al. *Genome Res.* **2005**, *15*, 1325.

(9) Griffiths, P. R.; Pariente, G. L. *Trends Anal. Chem.* **1986**, *5*, 209.

(10) Sali, A.; Blundell, T. L. *J. Mol. Biol.* **1993**, *234*, 779.

(11) Legler, P. M.; Kumaran, D.; Swaminathan, S.; Studier, F. W.; Millard, C. B. *Biochemistry* **2008**, *47*, 9592.

(12) Berman, H.; Henrick, K.; Nakamura, H.; Markley, J. L. *Nucleic Acids Res.* **2007**, *35* (Database Issue), D301.

(13) Altschul, S. F.; Madden, T. L.; Schäffer, A. A.; Zhang, J.; Zhang, Z.; Miller, W.; Lipman, D. J. *Nucleic Acids Res.* **1997**, *25*, 3389.

(14) Karplus, K.; Karchin, R.; Draper, J.; Casper, J.; Mandel-Gutfreund, Y.; Diekhans, M.; Hughey, R. *Proteins* **2003**, *53* (Suppl. 6), 491.

(15) Shi, J.; Blundell, T. L.; Mizuguchi, K. *J. Mol. Biol.* **2001**, *310*, 243.

(16) The UniProt Consortium. The Universal Protein Resource (UniProt) 2009. *Nucleic Acids Res.* **2009**, *37* (Database Issue), D169.

(17) Notredame, C.; Higgins, D. G.; Heringa, J. *J. Mol. Biol.* **2000**, *302*, 205.

(18) Rost, B.; Yachdav, G.; Liu, J. *Nucleic Acids Res.* **2004**, *32* (Web Server Issue), W321.

(19) Kabsch, W.; Sander, C. *Biopolymers* **1983**, *22*, 2577.

(20) Laskowski, R. A.; MacArthur, M. W.; Moss, D. S.; Thornton, J. M. *J. Appl. Crystallogr.* **1993**, *26*, 283.

(21) Sippl, M. *Proteins* **1993**, *17*, 355.

(22) Lindahl, E.; Hess, B.; van der Spoel, D. *J Mol. Model.* **2001**, *7*, 306.

(23) van der Spoel, D.; Lindahl, E.; Hess, B.; Groenhof, G.; Mark, A. E.; Berendsen, H. J. *J. Comput. Chem.* **2005**, *26*, 1701.

(24) van Gunsteren, W. F.; Billeter, S. R.; Eising, A. A.; Hunenberger, P. H.; Kruger, P.; Mark, A. E.; Scott, W. R. P.; Tironi, I. G. *Biomolecular Simulation: The GROMOS96 Manual and User Guide*; vdf Hochschulverlag AG an der ETH Zurich;: Zurich, Switzerland, 1996; p 1042.

(25) Berendsen, H. J. C.; Postma, J. P. M.; van Gunsteren, W. F.; Hermans, J. Interaction models for water in relation to protein hydration. In *Intermolecular Forces*; Pullman, B., Ed.; D. Reidel Publishing Company: Dordrecht, The Netherlands, 1981; p 331.

(26) Hess, B.; Bekker, H.; Berendsen, H. J. C.; Fraaije, J. G. E. M. *J. Comput. Chem.* **1997**, *18*, 1463.

(27) Berendsen, H. J. C.; Postma, J. P. M.; van Gunsteren, W. F.; Di Nola, A.; Haak, J. R. *J. Chem. Phys.* **1984**, *81*, 3684.

(28) Essmann, U.; Perera, L.; Berkowitz, M. L.; Darden, T.; Lee, H.; Pedersen, L. G. *J. Chem. Phys.* **1995**, *103*, 8577.

(29) McDonald, I. K.; Thornton, J. M. *J. Mol. Biol.* **1994**, *238*, 777.

(30) Kumar, S.; Nussinov, R. *J. Mol. Biol.* **1999**, *293*, 1241.

(31) Krimm, S.; Bandekar, J. *Adv. Protein Chem.* **1986**, *38*, 181.

(32) Byler, D. M.; Susi, H. *Biopolymers* **1986**, *25*, 469.

(33) Surewicz, W. K.; Mantsch, H. H. *Biochim. Biophys. Acta* **1988**, *952*, 115.

(34) Goormaghtigh, E.; Cabiaux, V.; Ruysschaert, J. M. Determination of soluble and membrane protein structure by Fourier transform infrared spectroscopy. III. Secondary structures. In *Physicochemical Methods in the Study of Biomembranes*; Subcellular Biochemistry Series; Hilderson, H. J., Ralstion, G. B., Eds.; Plenum Press: New York, 1994; Vol. 23, p 450.

(35) Alterio, V.; Aurilia, V.; Parracino, A.; Saviano, M.; Pedone, C.; Rossi, M.; D'Auria, S.; De Simone, G.Presented at the First Meeting of the Italian and Spanish Crystallographic Associations (MISCA) Copanello di Stalettì, Italy, Sep 24−28, 2006.

(36) Aurilia, V.; Parracino, A.; D'Auria, S. *Gene* **2008**, *410*, 234.

(37) Timasheff, S. N.; Susi, H.; Stevens, L. *J. Biol. Chem.* **1967**, *242*, 5467.

(38) Clark, A. H.; Saunderson, D. H.; Suggett, A. *Int. J. Pept. Protein Res.* **1981**, *17*, 353.

(39) Muga, A.; Surewicz, W. K.; Wong, P. T.; Mantsch, H. H. *Biochemistry* **1990**, *29*, 2925.

(40) Jackson, M.; Mantsch, H. H. *Biochim. Biophys. Acta* **1992**, *1118*, 139.

JP901921R